CORRELATED-ELECTRON THEORY OF METAMAGNETISM IN STRONGLY ANISOTROPIC ANTIFERROMAGNETS

K. HELD

Institut für Theoretische Physik C, RWTH Aachen, D-52056 Aachen, Germany

M. ULMKE* and D. VOLLHARDT

Institut für Festkörperforschung, Forschungszentrum Jülich, D-52425 Jülich, Germany

The electronic origin of metamagnetism in strongly anisotropic antiferromagnets is examined. To this end the infinite-dimensional Hubbard model with easy axis is investigated both analytically and numerically. At weak coupling a first order transition and at strong coupling a second order phase transition is found. To determine the transition behavior at intermediate coupling Quantum Monte Carlo techniques are used to calculate the field versus temperature phase diagram. The apparent similarities to the phase diagram of $FeBr_2$ and to mean field results for the Ising model with competing interactions are discussed.

1. Introduction

In 1939 Becquerel and van den Handel[1] reported the observation of an anomalous magnetization behavior in the mineral mesitite (carbonate of Fe and Mg) at low temperatures which they could not explain in terms of existing theories of magnetism. Therefore they suggested for it the name "metamagnetism".[2] Qualitatively similar, but even more drastic magnetization effects were later observed in many other systems of which $FeCl_2$ and $Dy_3Al_5O_{12}$ (DAG) are well-studied prototypes.[3] These materials are strongly anisotropic antiferromagnets where the spins are constrained to lie along an easy axis **e**. Under the influence of a strong magnetic field along **e** they undergo a first order ("metamagnetic"), rather than a spin-flop, transition from the antiferromagnetic (AF) to a paramagnetic state. Today the term "metamagnetic transition" is used in a much wider sense,[4] namely whenever $\chi(H)$ has a maximum at some value H_c, with $M(H)$ being strongly enhanced for $H > H_c$.[5] Metamagnetism is then found to be a rather common phenomenon which

*Present address: Physics Department, University of California, Davis, CA 95616, USA.

occurs also in strongly exchange-enhanced paramagnets (e.g. Ref. 4 $TiBe_2$, YCo_2), heavy fermion and intermediate valence systems (e.g. $CeRu_2Si_2$, UPt_3), and[5] the parent compound of high-T_c superconductivity (La_2CuO_4).

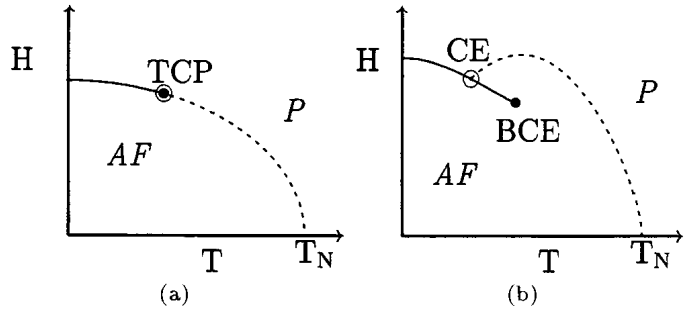

Fig. 1. Schematic $H-T$ phase diagram for (a) a typical Ising-type metamagnet (TCP: tricritical point), (b) the Ising model (1) in mean field theory with $R < 3/5$ (CE: critical endpoint, BCE: bicritical endpoint). Full lines: first order transition, broken lines: second order transition; AF: antiferromagnetic phase, P: paramagnetic phase.

In this paper we will be concerned only with metamagnetism in strongly anisotropic antiferromagnets, where a spin-flop transition does not occur. Apart from the well-known insulating materials, e.g. $FeCl_2$, there are also conducting materials, e.g. $UA_{1-x}B_x$ (where A = P, As; B = S, Se),[3] $SmMn_2Ge_2$[6] and $TbRh_{2-x}Ir_xSi_2$[7] in this group. Theoretical investigations of metamagnetism in these systems were so far restricted to the insulating systems, several of which are known to have a very interesting H–T phase diagram (H: *internal* magnetic field, T: temperature). In particular, it includes a tricritical point (TCP) at which the first order phase transition becomes second order (Fig. 1(a)) — a feature very similar to that found in ^{3}He–^{4}He mixtures.[8,9] Theoretical investigations of the multicritical behavior are usually based on the Ising model with more than one interaction in a magnetic field, on a simple cubic lattice,[9] e.g.

$$H = J \sum_{\text{N.N.}} S_i S_j - J' \sum_{\text{N.N.N.}} S_i S_j - H \sum_i S_i \,. \tag{1}$$

For $J, J' > 0$ one has an AF coupling between the Z nearest-neighbor (N.N.) spins and a ferromagnetic coupling between the Z' next-nearest-neighbors (N.N.N.).[10] It was pointed out by Kincaid and Cohen[11] that in mean field theory a TCP as in Fig. 1(a) exists only for $R \equiv Z'J'/(ZJ) > 3/5$, while for $R < 3/5$ this point separates into a critical endpoint (CE) and a bicritical endpoint (BCE) (see Fig. 1(b)). The latter behavior, especially the finite angle between the two transition lines at CE and the pronounced maximum at the second order line, is qualitatively very similar to that observed in $FeBr_2$.[12] However, the first order line between CE and BCE has so far not been observed — neither experimentally, nor even theoretically when evaluating (1) beyond mean field theory.[13,14] Most recently, by measurement of the excess magnetization and anomalous susceptibility loss, a strip-shaped regime

of strong *non-critical* fluctuations in the $H_a - T$ plane (where H_a is the applied field) of $FeBr_2$ was reported[15] which is at least reminiscent of the *critical* line CE $\leftrightarrow$ BCE. This unusual behavior was then also found theoretically by Selke and Dasgupta[16] who evaluated (1) in the limit of weak ferromagnetic coupling ($J'/J = 0.2$) and large Z using Monte Carlo techniques.

It is the purpose of this paper to go beyond an effective, classical Ising-spin model and to investigate the origin of metamagnetism in strongly anisotropic antiferromagnets from a microscopic point of view. Our question is: Which is the *minimal electronic correlation model* for metamagnetism in these systems? Since the Hubbard model at half-filling ($n = 1$) is the generic microscopic model for antiferromagnetism (both of itinerant and localized nature) in correlated electron systems, we will study this model. For nearest-neighbor hopping of electrons on a bipartite lattice in the presence of a magnetic field it has the form

$$\hat{H} = -t \sum_{\text{N.N.},\sigma} \hat{c}^{+}_{i\sigma} \hat{c}_{j\sigma} + U \sum_{i} \hat{n}_{i\uparrow} \hat{n}_{i\downarrow} - \sum_{i\sigma} (\mu + \sigma H) \hat{n}_{i\sigma} \ , \tag{2}$$

where operators carry a hat. In this paper we consider a half-filled band in which case $\mu = U/2$ by particle–hole symmetry. From the exact, analytic solution in dimensions $d = 1$ the (paramagnetic) ground state of this model is known to exhibit metamagnetic behavior, i.e. $\partial\chi/\partial H > 0$ up to saturation.[17] The only other dimension in which the dynamics of the correlation problem can be treated exactly in the thermodynamic limit is $d = \infty$.[18] In this limit, with the scaling $t = t^*/\sqrt{Z}$ in (2), one obtains a dynamical single-site problem[19] which is equivalent to an Anderson impurity model complemented by a self-consistency condition,[20] and is thus amenable to numerical investigations within a finite-temperature Monte-Carlo approach.[21] This approach has recently provided valuable insight into the physics of strongly correlated electron systems, e.g. the Mott–Hubbard transition[22] and transport properties.[23] The effect of the magnetic field H in (2) for $n = 1$ was also studied.[24–26] In particular, Laloux *et al.*[26] thoroughly investigated the magnetization behavior of the paramagnetic phase, assuming the AF order to be suppressed. For $U = 3\sqrt{2}t^*$ they find a first order metamagnetic transition between the strongly correlated metal and the Mott-insulator at a critical field $H \simeq 0.2t^*$. Giesekus and Brandt[24] also took into account the AF order. They considered the case where the field $\mathbf{H}$ orients the staggered magnetization $\mathbf{m}_{\text{st}}$ perpendicular to itself. For isotropic antiferromagnets this is indeed the arrangement with lowest energy. There is then no metamagnetism.

To investigate how metamagnetism may arise in correlated electron systems with strongly *anisotropic* AF order we will work in the AF phase of the Hubbard model, too, but will constrain $\mathbf{m}_{\text{st}}$ to lie *parallel* to $\mathbf{H}$. In this way the existence of an easy axis $\mathbf{e}$ along which $\mathbf{H}$ is directed, such that $\mathbf{e} \parallel \mathbf{m}_{\text{st}} \parallel \mathbf{H}$, is incorporated in a natural way.[27] We will first discuss (2) in the limit of strong and weak coupling since this will already show that the appearance of a tri- or multicritical point is a delicate matter.

1. Strong coupling: In the limit $U \gg t$ the Hubbard model at $n = 1$ is equivalent to an effective Heisenberg spin-model, $\hat{H}_{\text{Heis}} = J \sum_{\text{N.N.}} \sum_{\alpha=x,y,z} \hat{S}_i^\alpha \hat{S}_j^\alpha - H \sum_i \hat{S}_i^z$, with an AF exchange coupling $J = 4t^2/U$. For this model Weiss mean field theory becomes exact in $d = \infty$ yielding the same results as for the Ising model (1) with $J' = 0$.[28] In this case the transition line in the H–T phase diagram has indeed the form shown in Fig. 1(a) — *but it is of second order for all* $T > 0$, i.e. $T_t = 0$. The behavior changes if we include the next term in the effective spin-Hamiltonian, of order t^4/U^3, involving two- and four-spin terms.[29] The latter lead to an effective ferromagnetic spin coupling J'. Then we obtain essentially the mean field theory for the Ising model (1) with $J = 4t^2/U$ and $J' \propto (t/U)^2 J \ll J$, and thus expect to find the transition scenario in Fig. 1(b). However, since the expansion is in $t/U \ll 1$ it is not *a priori* clear down to what values of U/t this behavior can actually be observed.

2. Weak coupling: For $U \ll t$ we expect the Hartree–Fock approximation, a *static* mean field theory, to give an, at least, qualitatively correct answer. Within this approximation and for $\mathbf{m}_{\text{st}} \parallel \mathbf{H}$[27] we find a metamagnetic phase transition, too — *but it is of first order for all* T *and* U, corresponding to Fig. 1(a), but with $T_t = T_{\text{N}}$. Hence the Hartree-Fock solution cannot describe the experimental situation. Apparently the location of the (tri-) critical point in the H–T phase diagram, and even the transition scenario itself, depends sensitively on the value of the electronic on-site interaction U. To study this point in greater detail we have to go to intermediate coupling.

3. Intermediate coupling: In this interaction range we solve (2) numerically in $d = \infty$. In contrast to Hartree–Fock this limit provides a *dynamic* mean field theory. The local self-energy $\Sigma_{\alpha n}^\sigma$ and propagator $G_{\alpha n}^\sigma$, where the subscript n denotes the Matsubara frequency $\omega_n = (2n+1)\pi T$ and $\alpha \in (A, B) = (+, -)$ is the sublattice index, are determined by two sets of dynamically coupled, self-consistent equations for G and Σ[19,20,30]:

$$G_{\alpha n}^\sigma = \int_{-\infty}^{\infty} d\epsilon \frac{N^0(\epsilon)}{z_{\alpha n}^\sigma - \epsilon^2 / z_{-\alpha n}^\sigma} = -\langle \psi_{\sigma n} \psi_{\sigma n}^* \rangle_{A_\alpha} \,. \tag{3}$$

Here $z_{\alpha n}^\sigma = i\omega_n + \mu - \Sigma_{\alpha n}^\sigma$, and the thermal average in (3) is defined as a functional integral over the Grassmann variables ψ, ψ^*, with $\langle \mathcal{O} \rangle_{A_\alpha} = \int \mathcal{D}[\psi] \mathcal{D}[\psi^*] \times \mathcal{O} e^{A_\alpha\{\psi,\psi^*,\Sigma,G\}} / Z_\alpha$, in terms of the single-site action

$$A_\alpha = \sum_{\sigma,n} \psi_{\sigma n}^* \left[(G_{\alpha n}^\sigma)^{-1} + \Sigma_{\alpha n}^\sigma \right] \psi_{\sigma n} - U \int_0^\beta d\tau \psi_\uparrow^*(\tau) \psi_\uparrow(\tau) \psi_\downarrow^*(\tau) \psi_\downarrow(\tau) \,, \tag{4}$$

with Z_α as the partition function. Furthermore $N^0(\epsilon)$ is the density of states of the non-interacting electrons. As the results do not much depend on its precise form we choose $N^0(\epsilon) = [(2t^*)^2 - \epsilon^2]^{1/2} / (2\pi t^{*2})$. From now on we will set $2t^* \equiv 1$, i.e. measure all energies in units of half the band width. For finite T and not too large U the functional integral can be calculated numerically by Quantum Monte

Carlo simulations.[21,30] Equation (3) is solved by iteration. All calculations were performed for $U = 2$ (= band width) where the Néel temperature in zero field is close to its maximum value $T_{\mathrm{N,\,max}} = 0.10$.[31]

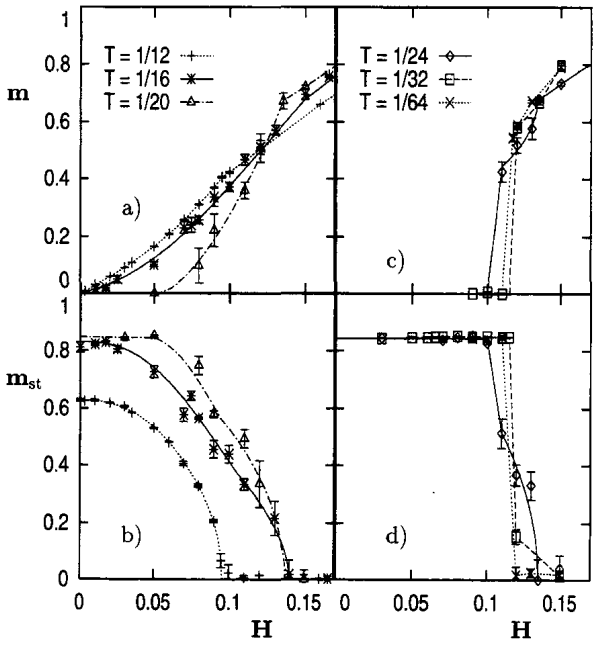

Fig. 2. QMC-results, including error bars, for the magnetization $m(H)$ and staggered magnetization $m_{\mathrm{st}}(H)$ as obtained for the $d = \infty$ Hubbard model with easy axis along H at $n = 1$ and $U = 2$ for two sets of temperatures. Curves are guides to the eye only.

The results for the magnetization $m(H)$ and the staggered magnetization $m_{\mathrm{st}}(H)$[32] are shown in Fig. 2. The metamagnetic behavior is clearly seen: at $T = 1/12$ $m(H)$ begins to show a typical "S-shape" which becomes more pronounced at $T = 1/16$ (Fig. 2(a)). For these temperatures m_{st} is a continuous function of H (Fig. 2(b)), which vanishes at the critical field H_{c} as $m_{\mathrm{st}} \sim (H_{\mathrm{c}} - H)^{\nu}$. A least-square fit through five points (weighted with the error bars) near the transition yields $\nu = 0.46 \pm 0.05$ for $T = 1/12$, which is compatible with a mean field exponent $\nu = 1/2$. By contrast, at the lowest temperatures, $T \leq 1/32$ (Figs. 2(c) and (d)) the transitions in m and m_{st} are clearly discontinuous. Hysteresis is only weak and is not shown. The field dependence at intermediate temperatures $1/16 < T < 1/32$ is more complex: m_{st} is almost field-independent (i. e. $m \simeq 0$) below some field H_{c}', decreases sharply at H_{c}' (such that $m > 0$), but vanishes only at a field $H_{\mathrm{c}} > H_{\mathrm{c}}'$ in a continuous way. Although the error bars do not permit an unambiguous interpretation it seems that the order parameter decreases by *two* consecutive transitions: the first one, at H_{c}', being of first order or an anomaly and the second one, at H_{c}, of second order.

The results for $m(H)$ and $m_{\rm st}(H)$ are used to construct the H–T phase diagram shown in Fig. 3. It displays all the features of Fig. 1(b). In particular, the first order line, defined by $H_{\rm c}'(T)$ for $T > T_{\rm CE}$, continues *into* the ordered phase, separating two different AF phases: AF_I (where $m \simeq 0$) and AF_{II} (where $m > 0$). The position of its endpoint cannot, at present, be determined accurately (dotted line). We note that the ratio of $T_{\rm CE}$ and the Néel temperature $T_{\rm N}$ at $H = 0$ is $T_{\rm CE}/T_{\rm N} \simeq 0.3$.

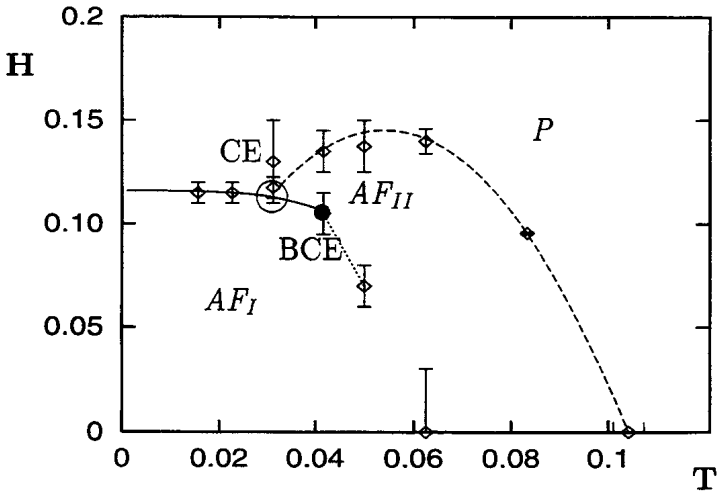

Fig. 3. H–T phase diagram for the $d = \infty$ Hubbard model with easy axis along H at $n = 1$ and $U = 2$ as constructed from the QMC-results for $m(H)$ and $m_{\rm st}(H)$; same notation as in Fig. 1(b).

The H–T phase diagram in Fig. 3 is strikingly similar to the experimental phase diagram of $FeBr_2$,[15,33] although in this system one should expect U to be much larger than the band width. In particular, the part of the first order line extending into the ordered phase clearly resembles the regime where an anomalous, but *non-critical*, behavior was observed.[15] It appears that there may well exist a truely *critical* feature in this part of the H–T (rather than $H_a - T$) phase diagram. It would therefore be interesting to measure $m_{\rm st}(T, H)$ in $FeBr_2$ by neutron scattering to see whether such a feature really exists. The results shown in Figs. 2 and 3 are qualitatively very similar to the mean field solution of the Ising model (1) with $J' \ll J$.[11,14] The applicability of mean field theory itself to $FeBr_2$ seems to be justified by the fact that in this material the AF superexchange involves 20 equivalent sites in the two neighboring iron planes.[34] We note that in $FeBr_2$ $T_{\rm CE}/T_{\rm N} = 0.33$.[12]

In summary, we investigated the origin of metamagnetism in strongly anisotropic antiferromagnets starting from a microscopic model of strongly correlated-electrons, the Hubbard model with easy axis, in a dynamical mean field theory. The H–T phase diagram obtained for an intermediate on-site interaction ($U = 2$ = band width) is qualitatively very similar to that of $FeBr_2$. Apart from calculations at $U < 2$, it will be interesting to calculate off half-filling. This will allow us to investigate

the properties of metallic metamagnets, such as the Uranium-based mixed-systems, for which a theory in terms of an itinerant electron model is mandatory.

Acknowledgment

We acknowledge useful correspondence with N. Giordano, G. Lander, B. Lüthi, A. Ramirez, and W. Wolf, and are grateful to H. Capellmann, P. van Dongen, W. Metzner, H. Müller-Krumbhaar, F. Steglich, G. Stewart and, in particular, to V. Dohm, W. Kleemann and W. Selke for very helpful discussions. This work was supported in part by the SFB 341 of the DFG and by a grant from the Office of Naval Research, ONR N00014-93-1-0495.

References

1. J. Becquerel and J. van den Handel, *J. de Physique et le Radium* **10**, 10 (1939).
2. This name was apparently coined by H. A. Kramers; see J. Becquerel, in *Le Magnétisme* (Institut International de Cooperation Intellectuelle, CNRS, Paris, 1940), p. 97.
3. For a review see E. Stryjewski and N. Giordano, *Adv. Phys.* **26**, 487 (1977).
4. F. Acker *et al.*, *Phys. Rev.* **B24**, 5404 (1981); T. Sakakibara *et al.*, *J. Phys.: Condens. Matter* **2**, 3381 (1990).
5. For a review see B. Lüthi *et al.*, *J. Magn. Magn. Mat.* **90 & 91**, 37 (1991).
6. J. H. V. J. Brabers *et al.*, *Phys. Rev.* **B50**, 16410 (1994).
7. V. Ivanov *et al.*, *J. Alloys Comp.* **218**, L19 (1995).
8. R. B. Griffiths, *Phys. Rev. Lett.* **24**, 715 (1970).
9. For a review see I. D. Lawrie and S. Sarbach, in *Phase Transitions and Critical Phenomena, Vol. 9*; eds. C. Domb and J. L. Lebowitz (Academic Press, New York, 1984), p. 1.
10. This Hamiltonian allows one to study metamagnetism in strongly anisotropic antiferromagnets such as $FeCl_2$, $FeBr_2$, which are layered materials with ferromagnetic interactions within the plane and antiferromagnetic interactions between the planes. Adjacent layers belong to different sublattices. Note that for $J, J' > 0$ both interactions in (1) *favor* antiferromagnetic ordering on N.N. sites.
11. J. M. Kincaid and E. G. D. Cohen, *Phys. Lett.* **50A**, 317 (1974); J. M. Kincaid and E. G. D. Cohen, *Phys. Rep.* **22**, 57 (1975).
12. A. R. Fert *et al.*, *J. Phys. Chem. Solids* **34**, 223 (1973); C. Vettier, H. L. Alberts, and D. Bloch, *Phys. Rev. Lett.* **31**, 1414 (1973).
13. H. J. Herrmann and D. P. Landau, *Phys. Rev.* **B48**, 239 (1993).
14. W. Selke, private communication.
15. M. M. P. de Azevedo *et al.*, *J. Magn. Magn. Mater.* **140–144**, 1557 (1995); J. Pelloth *et al.*, *Phys. Rev.* **B52**, 15372 (1995).
16. W. Selke and S. Dasgupta, *J. Magn. Magn. Mater.* **147**, L245 (1995); W. Selke, *Z. Phys.* **B** (in press).
17. M. Takahashi, *Prog. Theor. Phys.* **42** 1098 (1969).
18. W. Metzner and D. Vollhardt, *Phys. Rev. Lett.* **62**, 324 (1989); for a review see D. Vollhardt, in *Correlated Electron Systems*, ed. V. J. Emery (World Scientific, Singapore, 1993), p. 57.
19. V. Janiš, *Z. Phys.* **B83**, 227 (1991).
20. A. Georges and G. Kotliar, *Phys. Rev.* **B45**, 6479 (1992); M. Jarrell, *Phys. Rev. Lett.* **69**, 168 (1992).

21. J. E. Hirsch and R. M. Fye, *Phys. Rev. Lett.* **56**, 2521 (1986).
22. For a review see G. Kotliar, in *Strongly Correlated Electronic Materials*, eds. K. S. Bedell *et al.* (Addison-Wesley, Reading, 1994), p. 141.
23. For a review see Th. Pruschke, M. Jarrell, and J. K. Freericks, *Adv. Phys.* **44**, 187 (1995).
24. A. Giesekus and U. Brandt, *Phys. Rev.* **B48**, 10311 (1993).
25. T. Saso and T. Hayashi, *J. Phys. Soc. Jpn.* **63**, 401 (1994).
26. L. Laloux, A. Georges, and W. Krauth, *Phys. Rev.* **B50**, 3092 (1994).
27. At half-filling and for U equal to the band width, the difference between the free energy of the configuration with $\mathbf{m}_{\rm st} \parallel \mathbf{H}$ and $\mathbf{m}_{\rm st} \perp \mathbf{H}$, $F_{\parallel} - F_{\perp}$, does not exceed a few percent of the band width, i.e. $\mathcal{O}(10^{-2}$ eV), within Hartree–Fock. In this situation the spin-orbit interaction, which can be relatively strong, $\mathcal{O}(0.1\ eV)$, introduces a strong anisotropy, i.e. an easy axis $\hat{e}$ along which $\mathbf{m}_{\rm st}$ is rigidly fixed. Since the existence of $\hat{e}$ and the correlation physics described by (2) are quite unrelated it is justified to evaluate (2) under the constraint $\hat{e} \parallel \mathbf{m}_{\rm st} \parallel \mathbf{H}$.
28. In fact, the constraint of an uniaxial magnetization makes the Heisenberg model equivalent to the Ising model.
29. P. G. J. van Dongen, *Phys. Rev.* **B49**, 7904 (1994).
30. For details see M. Ulmke, V. Janiš, and D. Vollhardt, *Phys. Rev.* **B51**, 10411 (1995); all calculations were performed on a Cray YMP of the Forschungszentrum Jülich.
31. The constraint $\mathbf{m}_{\rm st} \parallel \mathbf{H}$ is enforced by setting the off-diagonal (in spin space) elements of the propagator equal to zero: $\langle \psi_\alpha^\downarrow \psi_\alpha^{\uparrow *} \rangle = 0$.
32. Here m and $m_{\rm st}$ are defined in terms of the sublattice magnetization $m_\gamma = (2/L) \sum_{i \in \gamma} \langle \hat{n}_{i\uparrow} - \hat{n}_{i\downarrow} \rangle$, with $\gamma = A$ or B, and L as the number of lattice sites, by $m = (m_A + m_B)/2$ and $m_{\rm st} = (m_A - m_B)/2$.
33. Note that the mixed-phase region in the phase diagram of Ref. 12 disappears when instead of the applied field H_a the internal field H is plotted versus T.
34. L. Hernández, H. T. Diep, and D. Bertrand, *Europhys. Lett.* **21**, 711 (1993).